

## CORROSION PROPERTIES OF SELECTED ALUMINIUM ALLOYS IN MODEL ELECTROLYTES

Petra Lacková<sup>1)\*</sup>, Mária Hagarová<sup>1)</sup>, Jana Cervová<sup>1)</sup>, Ilija Mamuzić<sup>2)</sup>

<sup>1)</sup> Technical University of Košice, Faculty of Metallurgy, Košice, Slovakia

<sup>2)</sup> Croatian Metallurgical Society, Zagreb, Hrvatska

Received: 27.01.2014

Accepted: 28.03.2014

\*Corresponding author: e-mail: [petra.lackova@tuke.sk](mailto:petra.lackova@tuke.sk), Tel.: +421 55 602 2782, Department of Materials Science, Faculty of Metallurgy, Technical University of Košice, Letná 9, 042 00 Košice, Slovakia

### Abstract

The paper deals with the corrosion properties and corrosion resistance of aluminium alloys types of AlCu (EN AW 2017), AlMgSi (EN AW 6012) and AlZn (EN AW 7075) with heat treatment T3 (solution treatment, forming and natural aging). The basic corrosion characteristics were quantified by measurement of corrosion potential measured against the saturated calomel electrode and weight losses of exposed samples in the environment of distilled water and in solution SARS. The samples of aluminium alloys were immersed in above-mentioned environments for one minute for a period of six months. Furthermore, an extra evaluation of corrosion of exposed aluminium samples was carried out by means of metallographic analysis. The exposed sample surfaces were evaluated using a microscope.

**Keywords:** corrosion, resistance, potential, aluminium alloys

### 1 Introduction

Aluminium alloys are used mainly in aerospace and automobile industry where, except good mechanical features, high corrosion resistance to atmospheric conditions is required. Pure aluminium (99,5 %) has a high corrosion resistance which can be compared to aluminium alloys (in case they do not contain Cu). Resistance of aluminium and its alloys is associated with the formation of a protective layer of oxides, or aluminium hydroxides on their surface. Corrosion resistance depends on variety of factors, for example presence of cations and anions in solution, amount of oxygen, temperature and so on [1-4].

Corrosion damage of aluminium alloys may (depending on conditions) take place via spots, pitting or intergranular corrosion (degradation). In case of stress corrosion cracking appears [5-7].

In AlMgSi aluminium alloys the intergranular corrosion damage is caused by anodic dissolution of intermetallic phases Mg<sub>2</sub>Si on grain boundaries. Microgalvanic link between the accrued phases of Al<sub>2</sub>Cu, CuSi, MgSiCu, Mg<sub>2</sub>Si ( $\beta$ ) and pure silicon causes intergranular attack of the alloy due to the differences of potentials with the matrix. The corrosion resistance AlMgSi aluminium alloy also influences Cu content and Mg:Si ratio. AlZn alloys are susceptible to corrosion cracking in the presence of chlorides in corrosive environments and their high firmness. The development of microgalvanic link between the precipitate on the boundaries of grains and matrix is represented by an alloy also susceptible to intergranular corrosion. Low

corrosion resistance of AlCu alloys is caused by the presence of the main alloy element - Cu. The increase of copper in the precipitates causes depletion of copper leading to intergranular cracking [8-16].

## 2 Experimental material and methodology of experiments

Aluminium alloys EN AW 2017 (AlCu), EN AW 6012 (AlMgSi) and EN AW 7075 (AlZn) were used in order to perform all experiments. Chemical composition of these alloys is given in Table 1. Aluminium alloys were in the shape of bars and their structure corresponded to their heat treatment which also consisted of solution treatment, forming and natural aging. The samples used for metallographic analysis were prepared via a standard metallographic practice (grinding, polishing and etching in  $\text{HNO}_3 + \text{HF} + \text{distilled water}$ ). All the samples were observed and documented using a light microscope OLYMPUS VANOX-T.  $E_{\text{SCE}}$  corrosion potentials were determined on the samples which were measured against the saturated calomel electrode  $E_{\text{SCE}}$  using a milivolt Hgilent 34405A. Aluminium samples were immersed in distilled water and SARS (0,01 mmMol  $\text{HNO}_3$ ; 1 mmMol NaCl; 1 mmMol  $(\text{NH}_4)_2\text{SO}_4$ ) for over a six-month period.

## 3 Results and discussion

The surface of probationary samples before the corrosion test is documented in **Fig. 1**. The structure aluminium alloys is characterized by aluminium matrix with particles of intermetallic phases:  $\text{Al}_2\text{Cu}$  phase in the AlCu alloy,  $\text{Mg}_2\text{Si}$  phase in the AlMgSi alloy and  $\text{MgZn}_2$ ,  $\text{Al}_2\text{CuMg}$  phase in the AlZn alloy [17-20].

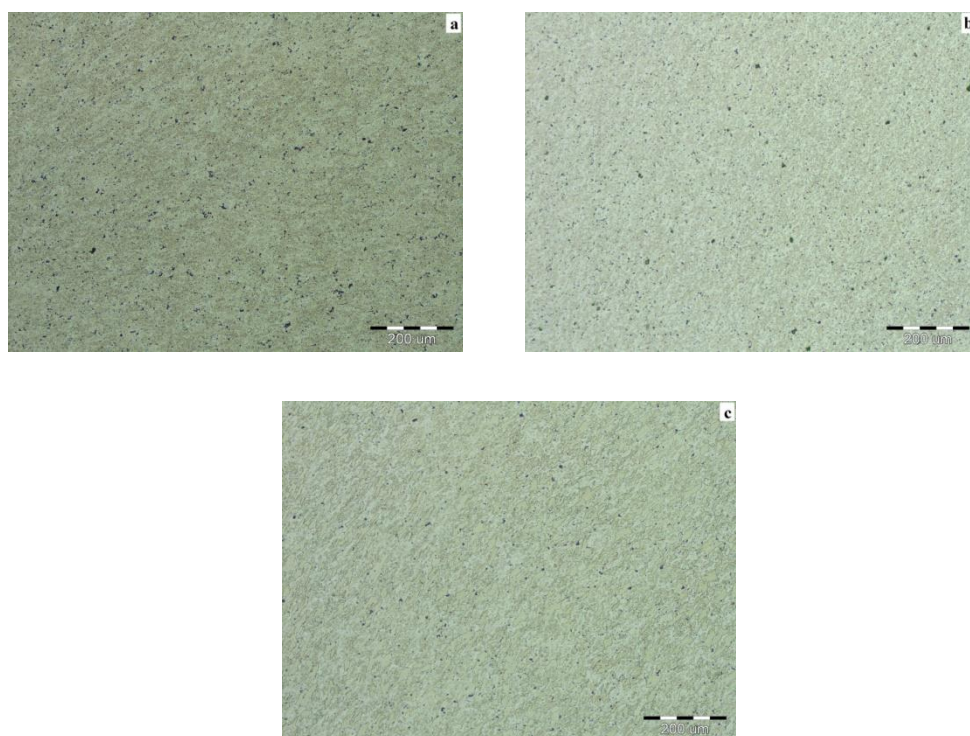


**Fig. 1** Structure of aluminium alloys: a) EN AW 2017, b) EN AW 6012, c) EN AW 7075

**Table 1** Chemical composition of aluminium

Material	Zn	Cu	Fe	Mg	Mn	Si
EN AW 2017	0.20	4.29	0.31	0.71	0.52	0.56
EN AW 6012	0.30	0.10	0.37	0.66	0.58	0.95
EN AW 7075	7.03	2.15	0.14	2.53	0.02	0.06

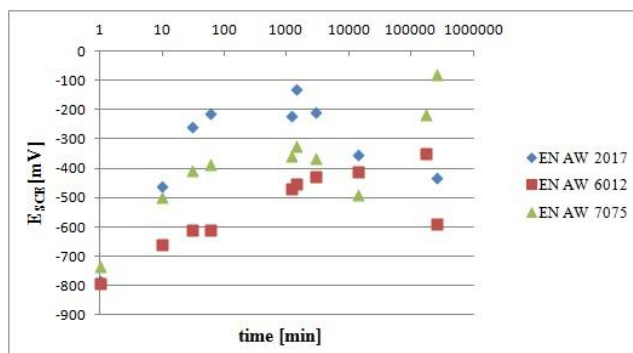
The measured corrosion potentials of  $E_{SCE}$  in the environment of distilled water and SARS are presented in **Table 2** and **Table 3**. **Fig. 2** and **Fig. 3** show process of fixation of the corrosion potentials during the exposition for particular samples exposed in a given corrosive environment. In all applied cases increased values of free corrosive potentials of the samples.

**Table 2** Corrosion potential  $E_{SCE}$  of aluminium alloys in distilled water

Material	Exposure time								
	1 [min]	10 [min]	30 [min]	1 [h]	24 [h]	48 [h]	10 [day]	4 [month]	6 [month]
<b>Corrosion potential <math>E_{SCE}</math> [mV]</b>									
EN AW 2017	- 783	- 462	- 260	- 214	- 131	- 208	- 355	- 349	- 434
EN AW 6012	- 792	- 662	- 610	- 610	- 455	- 428	- 414	- 350	- 591
EN AW 7075	- 736	- 501	- 410	- 387	- 325	- 368	- 491	- 216	- 80

**Table 3** Corrosion potential  $E_{SCE}$  of aluminium alloys in SARS

Material	Exposure time								
	1 [min]	10 [min]	30 [min]	1 [h]	24 [h]	48 [h]	10 [day]	4 [month]	6 [month]
<b>Corrosion potential <math>E_{SCE}</math> [mV]</b>									
EN AW 2017	- 867	- 503	- 430	- 417	- 420	- 404	- 385	- 521	- 495
EN AW 6012	- 966	- 809	- 730	- 681	- 612	- 564	- 571	- 580	- 614
EN AW 7075	- 607	- 600	- 578	- 552	- 549	- 566	- 554	- 559	- 566

**Fig. 2** Dependence of corrosion potential  $E_{SCE}$  on the exposure time of samples in distilled

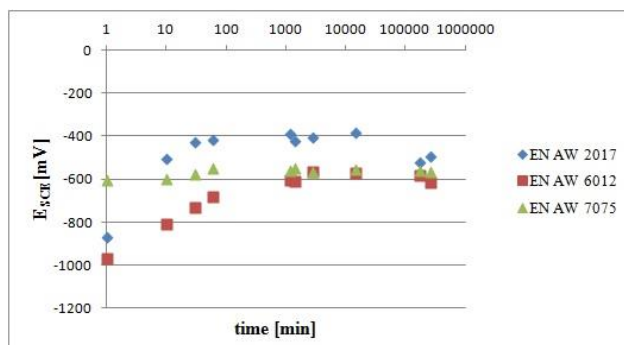


**Fig. 3** Dependence of corrosion potential  $E_{SCE}$  on the exposure time of samples in SARS

Based on the above mentioned dependences it may be stated that the  $E_{SCE}$  corrosion potential becomes less negative with the increasing time of exposure. This applies to all tested samples in both corrosion environments. In this case, the protective nature of the emergent layer of aluminium oxide, or aluminium hydroxide, started to appear on the surface. After a six-month exposure in distilled water the highest protective efficiency was achieved leading to the formation of a layer of corrosion products on the Al-Zn alloy whereas the value of potential reached up to  $-80$  mV in comparison to its initial value  $-736$  mV. In the environment of SARS, the best result was achieved in the sample of Al-Cu whereas the potential value after six months reached  $-495$  mV from the initial value  $-867$  mV.

Mass changes  $\Delta m$  of the corroded aluminium samples in corrosive environments during model corrosive laboratory test are shown in the chart **Table 4** and **Table 5**, their graphic representation is on **Fig. 4** and **Fig. 5**. Smallest corrosion changes of the mass were detected in both corrosive environments in alloys AlMgSi. In comparison to exposures in distilled water, greater corrosion weight loss was observed in all samples in solution SARS, regardless of their chemical composition.

**Table 4** Weight change  $\Delta m$  of samples during the time exposure in distilled water

Material	$\Delta m$ [g] / Distilled Water		
	Exposure Time [day]		
	10	120	181
EN AW 2017	75.42	35.92	41.20
EN AW 6012	0.002	0.01	0.05
EN AW 7075	3.21	46.29	43.82

**Table 5** Weight change  $\Delta m$  of samples during the time exposure in SARS

Material	$\Delta m$ [g] / SARS		
	Exposure Time [day]		
	10	120	181
EN AW 2017	156.86	24.34	66.26
EN AW 6012	0.001	0.004	0.35
EN AW 7075	4.64	151.23	96.55

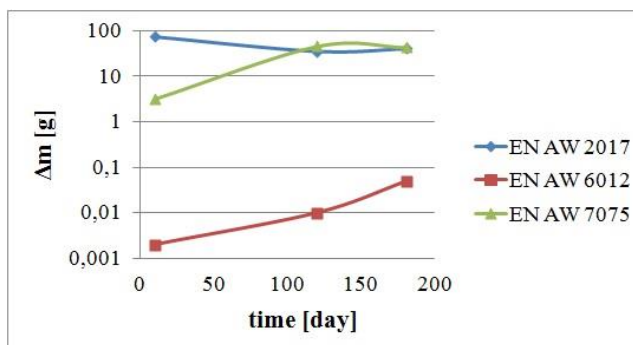


**Fig. 4** Weight change  $\Delta m$  of samples (aluminium alloys) after exposure time in distilled water

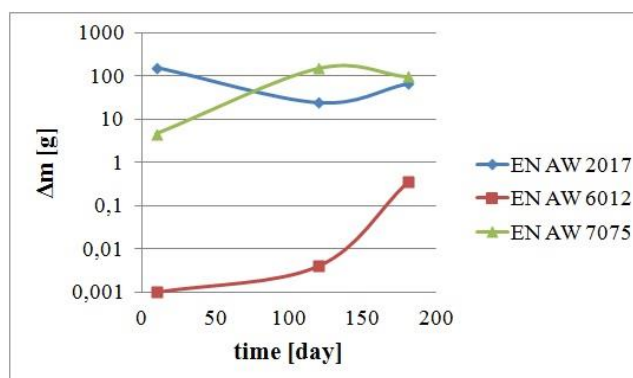


**Fig. 5** Weight change  $\Delta m$  of samples (aluminium alloys) after exposure time in SARS

The surface of all exposed samples after the removal of corrosion products was evaluated via the metallographic analysis bating, the results are documented in **Fig. 6** to **Fig. 11**.

The surface of all exposed samples was locally degraded by the corrosion with a different depth of attack. After a six-month exposure in the environment of distilled water, the surface of AlCu and AlZn alloys was more degraded, Fig. 6 and Fig. 11, leading to a bigger depth attack on their surfaces, appr. up to 100  $\mu\text{m}$ . As documented in Fig. 8 and Fig. 9, the microgeometry of the AlMgSi surface was changed only slightly, depth did not exceed the  $\mu\text{m}$  unit.

The rate of attack of aluminium alloys in the environment of SARS, Fig. 7, Fig. 9 and Fig. 11, was similar to the environment of distilled water. The least significant changes on the surface, corresponding to the loss of weight  $\Delta m$  reaching 0.05 g were documented on the AlMgSi sample, Fig. 8 to Fig. 9. On the other hand, the sample of Al-Cu was significantly damaged on several places, whereas the maximum depth of corrosion was up to about 100  $\mu\text{m}$  (shown in Fig. 6 to Fig. 7). The highest value of weight change  $\Delta m$  reaching 96.55 g corresponded to a higher number of corrosion holes on the surface of the AlCu alloy.

The visible compression effect on the surface of samples is documented in Fig. 6 to Fig. 11 when the heated grains grow excessively and result in a coarse-grained structure; in our case reaching the thickness of approximately 100  $\mu\text{m}$ .

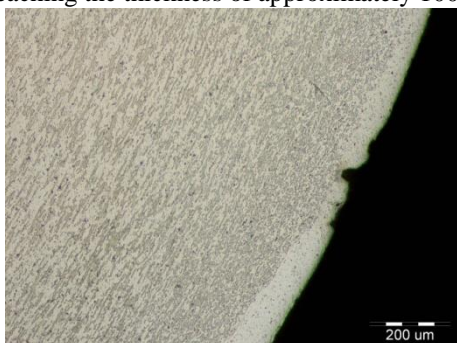


**Fig. 6** Surface of AlCu alloy after sixth months exposure in distilled water

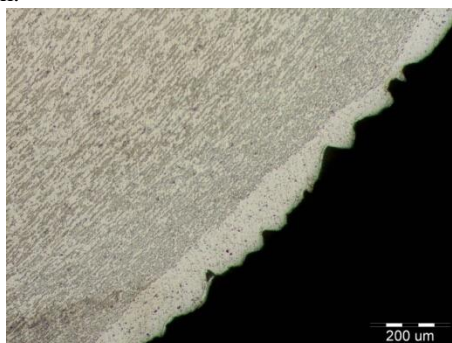


**Fig. 7** Surface of AlCu alloy after sixth months exposure in SARS

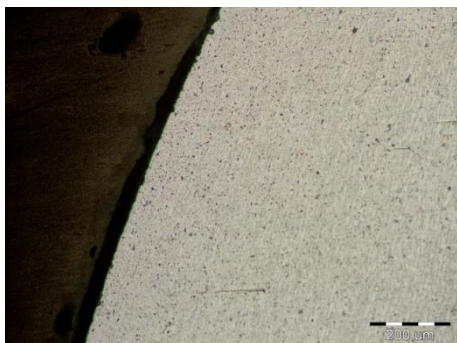


**Fig. 8** Surface of AlMgSi alloy after sixth months exposure in distilled water

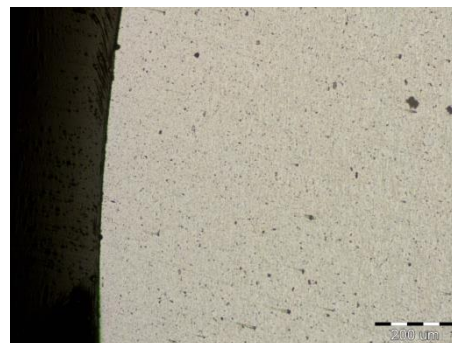


**Fig. 9** Surface of AlMgSi alloy after sixth months exposure in SARS

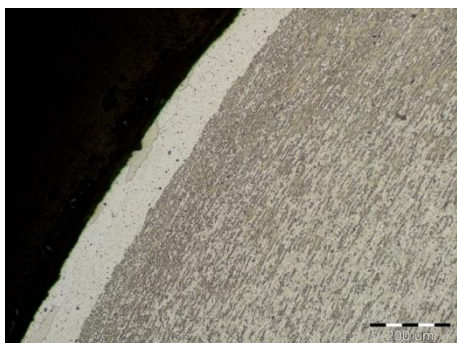


**Fig. 10** Surface of AlZn alloy after sixth months exposure in distilled water

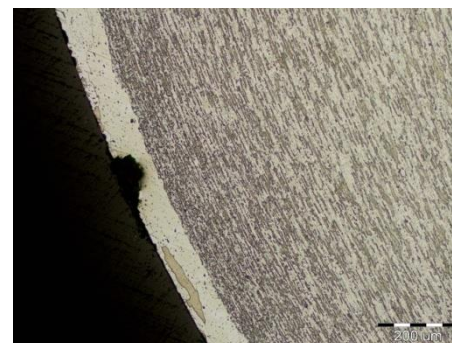


**Fig. 11** Surface of AlZn alloy after sixth months exposure in SARS

#### 4 Conclusions

Based on the metallographic analysis of surface exposed samples, measuring of corrosion potential  $E_{SCE}$  and mass changes  $\Delta m$  in distilled water and SARS can be observed the following facts: all aluminium alloys were attacked by pittings after six months of exposure in distilled water and SARS environment. The largest range of attack was observed on the Al-Cu alloy surface. The potential  $E_{SCE}$  of aluminium samples changed to a less negative values. The reason was formation of passive layer of corrosion products on their surface. This layer, however, did not provide sufficient protection against further corrosion process.

#### References

- [1] E. H. Hollingsworth, H. Y. Hunsicker: *Corrosion of Aluminum and Aluminum Alloys*. In: *Metals Handbook*, AMS International, Ohio, 1987, p. 583-609
- [2] J. Ševčíková: *Koroze hliníku a jeho slitin*. In: *Encyklopedie hliníku*, Adin, Prešov, 2005, p. 235-252 (in Czech)
- [3] CH. Vargel: *Corrosion of Aluminium*, eighth ed., Elsevier, Amsterdam, 2004
- [4] H. Zhan et al.: *Materials and Corrosion*, Vol. 59, 2008, No. 8, p. 670-675, doi: 10.1002/maco.200804110
- [5] S. Kale, V. Raja, A. Bakare: *Corrosion Science*, Vol. 75, 2013, p. 318-325, doi: 10.1016/j.corsci.2013.06.015
- [6] P. A. Schweitzer: *Metallic Materials, Physical, Mechanical, and Corrosion Properties*, first ed., M. Dekker, New York, 2003
- [7] M. Dekker: *Encyklopedia of Corrosion Technology*, second ed., New York, 2004
- [8] G. Svenningsen et al.: *Corrosion Science*, Vol. 48, 2006, No. 1, p. 226-242, doi: 10.1016/j.corsci.2004.11.025
- [9] A. El-Amoush: *Materials Chemistry and Physics*, Vol. 126, 2011, p. 607-613, doi: 10.1016/j.matchemphys.2011.01.010
- [10] G. Svenningsen, M. H. Larsen, J. H. Nordlien, K. Nisancioglu: *Corrosion Science*, Vol. 48, 2006, No. 12, p. 3969-3987, doi: 10.1016/j.corsci.2006.03.018
- [11] D. Litle, B. Connolly, J. Scully: *Corrosion Science*, Vol. 2, 2007, p. 347-372, doi: 10.1016/j.corsci.2006.04.024
- [12] T. Yue, L. Yan, C. Chan: *Applied Surface Science*, Vol. 14, 2006, p. 5026-5034, doi: 10.1016/j.apsusc.2005.07.052
- [13] F. Zeng et al.: *Transactions of Nonferrous Metals Society of China*, Vol. 12, 2011, p. 2559-2567, doi: 10.1016/S1003-6326(11)61092-3
- [14] K. Mroczka, A. Wójcicka, P. Kurtyka: *Acta Metallurgica Slovaca*, Vol. 18, 2012, No. 2-3, p. 82-91
- [15] W. Liang, P. Rometsch, L. Cao, N. Birbilis: *Corrosion Science*, Vol. 76, 2013, p. 119-128, doi: 10.1016/j.corsci.2013.06.035
- [16] E. Ghali: *Corrosion Resistance of Aluminum and Magnesium Alloys, Understanding, Performance, and Testing*, first ed., Wiley, New Jersey, 2010
- [17] L. Katgerman, D. Eskin: *Hardening, Annealing, and Aging*. In: *Handbook of Aluminum, Physical Metallurgy and Processes*, edited by G. E. Totten, D. S. MacKenzie, Dekker, New York, 2003, p. 259-303
- [18] M. Matvija et al.: *Acta Metallurgica Slovaca*, Vol. 18, 2012, No. 1, p. 4-12

- [19] M. Fujda, M. Matvija, T. Kvačkaj, O. Milkovič, P. Zubko, K. Nagyová: *Materiali in Tehnologije*, Vol. 46, 2012, p. 465-469
- [20] X. Li, M.J. Starink: *Materials Science and Technology*, Vol. 17, 2001, p. 1324-1328, doi:10.1179/026708301101509449

### **Acknowledgements**

*We would like to express our gratitude to doc. Ing. M. Škrobjan, PhD., and Ing. M. Bajcura PhD. who provided us with the experimental material.*